GASTROENTEROLOGY 2012;xx:xxx

Zinc Fingers and Homeoboxes 2 Inhibits Hepatocellular Carcinoma Cell Proliferation and Represses Expression of Cyclins A and E

XUETIAN YUE,* ZHENYU ZHANG,* XIAOHONG LIANG,* LIFEN GAO,* XIAONING ZHANG,* DI ZHAO,* XIAO LIU,* HONGXIN MA,* MIN GUO,* BRETT T. SPEAR,‡ YAOQIN GONG,§ and CHUNHONG MA*

*Key Laboratory for Experimental Teratology of Ministry of Education and Institute of Immunology, §Key Laboratory for Experimental Teratology of Ministry of Education and Institute of Genetics, Shandong University School of Medicine, Jinan, Shandong, People's Republic of China; ‡Department of Microbiology, Immunology, and Molecular Genetics and Markey Cancer Center, University of Kentucky College of Medicine, Lexington, Kentucky

BACKGROUND & AIMS: Zinc-fingers and homeoboxes 2 (ZHX2) represses transcription of several genes associated with liver cancer. However, little is known about the role of ZHX2 in the development of hepatocellular carcinoma (HCC). We investigated the mechanisms by which ZHX2 might affect proliferation of HCC cells. **METHODS:** We overexpressed and knocked down ZHX2 in HCC cells and analyzed the effects on proliferation, colony formation, and the cell cycle. We also analyzed the effects of ZHX2 overexpression in growth of HepG2.2.15 tumor xenografts in nude mice. Chromatin immunoprecipitation and luciferase reporter assays were used to measure binding of ZHX2 target promoters. Levels of ZHX2 in HCC samples were evaluated by immunohistochemistry. **RESULTS:** ZHX2 overexpression significantly reduced proliferation of HCC cells and growth of tumor xenografts in mice; it led to G1 arrest and reduced levels of Cyclins A and E in HCC cell lines. ZHX2 bound to promoter regions of *CCNA2* (which encodes Cyclin A) and *CCNE1* (which encodes Cyclin E) and inhibited their transcription. Knockdown of Cyclin A or Cyclin E reduced the increased proliferation mediated by ZHX2 knockdown. Nuclear localization of ZHX2 was required for it to inhibit proliferation of HCC cells in culture and in mice. Nuclear localization of ZHX2 was reduced in human HCC samples, even in small tumors (diameter, <5 cm), compared with adjacent nontumor tissues. Moreover, reduced nuclear levels of ZHX2 correlated with reduced survival times of patients, high levels of tumor microvascularization, and hepatocyte proliferation. **CONCLUSIONS: ZHX2 inhibits HCC cell proliferation by preventing expression of Cyclins A and E, and reduces growth of xenograft tumors in mice. Loss of nuclear ZHX2 might be an early step in the development of HCC.**

Keywords: Mouse Model; Carcinogenesis; shRNA; CCK-8.

Hepatocellular carcinoma (HCC) is the fifth most common cancer and the third most common cause of cancer deaths worldwide.[1] Environmental factors, most notably hepatitis B virus and hepatitis C virus infection and chronic alcohol exposure, are known risk factors of HCC development.[1,2] A number of genetic loci that contribute to HCC progression also have been identified.[2,3] Numerous studies have investigated transcriptional changes in HCC, including microarray analyses of global gene expression changes. Although differences in expression of a number of liver-enriched transcription factors have been reported, consistent differences have not always been observed and it is not clear which of these are relevant to HCC progression.[4] However, several genes that are expressed abundantly in the fetal liver, silenced at birth, and reactivated in HCC have been identified,[4] including *α-fetoprotein* (*AFP*), *H19*, and *glypican 3* (*GPC3*).[5–8] A better understanding of how these genes are reactivated in HCC may elucidate transcription changes that occur during liver cancer progression.

Although the *AFP*, *H19*, and *GPC3* genes are silenced at birth in most mouse strains, these 3 genes continue to be expressed in the adult liver of BALB/cJ mice.[9] Further studies indicated that the incomplete repression of these 3 genes in BALB/cJ mice is caused by a natural mutation in the *zinc fingers and homeoboxes 2* (*ZHX2*) gene.[9,10] More recent studies indicated that ZHX2 also regulates hepatic enzymes involved in plasma lipid homeostasis, including lipoprotein lipase.[11] ZHX2 is a member of a small family that also includes ZHX1 and ZHX3.[12–14] These proteins are predicted to contain 2 zinc-fingers and 4 or 5 homeodomains, motifs that could confer protein interaction and nucleic acid binding activities. The experiment of yeast 2-hybrid indicated that ZHX proteins can form homodimers as well as heterodimers with each other and with the A subunit of nuclear factor Y (NF-YA).[13–15] Current studies have suggested that ZHX proteins are expressed ubiquitously and found primarily in the nucleus, where they function as transcriptional repressors.[14,16] We previously showed that ZHX2 reduces AFP secretion[17] and GPC3 expression (unpublished data) in human HCC cell lines. Cotransfection assays by us and others also have shown that ZHX2 can repress the promoters of *AFP* and the NF-YA–regulated genes *cdc25C* and *Hexokinase II*.[14,17,18]

Abbreviations used in this paper: AFP, α-fetoprotein; ChIP, chromatin immunoprecipitation; CHO, Chinese hamster ovary; EGFP, enhanced green fluorescent protein; GPC3, glypican 3; HA, hemagglutinin; HCC, hepatocellular carcinoma; mRNA, messenger RNA; MVD, microvascular density; NF-YA, A subunit of nuclear factor Y; NLS, nuclear localization signal; PCR, polymerase chain reaction; shRNA, short hairpin RNA; siRNA, small interfering RNA; ZHX2, zinc-fingers and homeoboxes 2.

0016-5085/$36.00
http://dx.doi.org/10.1053/j.gastro.2012.02.049

Several studies investigating ZHX2 and HCC have provided conflicting data. By using methylation-sensitive restriction fingerprinting, Lv[19] et al showed hypermethylation of the *ZHX2* promoter in some HCC samples and HepG2 cells that correlated with the lack of ZHX2 expression. This silencing of expression suggests that ZHX2 might function as a tumor suppressor. In contrast, using immunohistochemical analysis, Hu et al[20] reported increased ZHX2 staining in HCC samples compared with normal liver; this study also noted higher ZHX2 expression in poorly differentiated and metastasis samples. These data are consistent with ZHX2 having tumor-promoting properties.

In the present study, we investigated the role of ZHX2 in the growth of liver cell lines both in vitro and in vivo. Our data showed that ZHX2 inhibits HCC cell growth. We also showed that ZHX2 represses Cyclin A and Cyclin E expression, which might account for the growth-inhibitory properties of ZHX2. Nuclear localization of ZHX2 is critical for its inhibitory effects. These data are supported by analysis of clinical samples, which show decreased nuclear expression of ZHX2 in HCC samples compared with adjacent nontumor tissue.

Materials and Methods

Cell Lines, Plasmids, and Small Interfering RNAs

The human HCC cell lines HepG2, SMMC7721, and QSG7701, Chinese hamster ovary (CHO) cells, and human embryonic kidney 293 cells were purchased from the Shanghai Cell Collection (Shanghai Institutes for Biological Sciences, Chinese Academy of Sciences, Shanghai, China). The HepG2.2.15 cell line was obtained from the Shandong Academy of Medical Sciences (Shandong, China). These cells were maintained as described previously.[17]

ZHX2 expression vectors pcZHX2 (full-length ZHX2 with a carboxy-terminal hemagglutinin [HA] tag cloned in pcDNA3.0) and pZHX2 (ZHX2–enhanced green fluorescent protein [EGFP] fusion protein) and short hairpin RNA (shRNA) vectors against human ZHX2 (pS1674, pS2360) were described previously.[17] Truncated forms of human ZHX2 containing homeodomain 1 and homeodomain 2 in which the nuclear localization signal (NLS) was present or absent (ZHX2[242–446] and ZHX2[242–439], respectively) were generated by polymerase chain reaction (PCR) amplification of pZHX2 using primers shown in Supplementary Table 1 and cloned into pEGFP-N1 (Invitrogen, Beijing, China). The luciferase reporter plasmids pGL3-Ap and pGL3-Ep were constructed by cloning the promoter regions of human *Cyclin A* (−505 to +361, the transcription initiation site designated as +1) and *Cyclin E* (−402 to +72), respectively, into the promoterless pGL3-basic vector (Promega).[21,22] The small interfering RNAs (siRNAs) against *Cyclin A*, *Cyclin E*, and *Cyclin D1* (Supplementary Table 2) were synthesized by the Shanghai Genepharma Co (Shanghai, China).

Analysis of Cell Proliferation, Cell Cycle, and In Vivo Tumor Growth

Cell viability was measured using the Cell Counting Kit-8 (CCK-8; Beyotime, Nanjing, China) and standard colony formation assays were used to measure cell proliferation. Each experiment was repeated 3–4 times. For cell-cycle analysis, cells were collected 48 hours after transfection with indicated plasmids, stained with propidium iodide (Sigma, St Louis, MO), and assayed using a Beckman Coulter Flow Cytometer (Fullerton, CA).

Male BALB/c nude mice (4–6 weeks of age) were purchased from the Animal Research Committee of the Institute of Biology and Cell Biology (Shanghai, China) and housed in the Shandong University School of Medicine animal facility according to protocols approved by the Shandong University Animal Care Committee. HepG2.2.15 cells (1×10^7) were transplanted subcutaneously into nude mice. After reaching a diameter of 0.5 cm, tumors were injected with plasmid (20 μg/100 μL) every fourth day for a total of 3–4 injections. Tumor size was monitored every other day. Mice were killed 4 days after the final injection and the tumors were isolated and weighed. Animal experiments were repeated at least twice and 6 mice were included in each cohort. Cell proliferation in each tumor was assayed by immunoperoxidase staining with an anti–Ki-67 antibody (ab15580; Abcam). Eight fields of roughly 1000 tumor cells for each section were scored independently by 3 pathologists.

Western Blotting

Cytoplasmic, nuclear, or whole-cell extracts were prepared and analyzed by Western blotting as previously described using anti-ZHX2 (Abcam), anti–Cyclin A (4656; Cell Signaling Technology, Danvers, MA), anti–Cyclin E (sc-25303; Santa Cruz Biotechnology, Santa Cruz, CA), anti–Cyclin D1 (ab6152; Abcam), anti-p21 (sc-6246; Santa Cruz Biotechnology), anti-p27 (ab32034; Abcam), anti-GFP (AG281; Beyotime), anti–histone H2A.X (BS5524; Bioworld Technology, Inc, St Louis Park, MN), anti–lamin A/C (BS1446; Bioworld Technology, Inc), and anti–β-actin (Sigma).[17]

Transfections, Fluorescent Staining, and Luciferase Assays

CHO and human embryonic kidney 293 cells transfected with indicated plasmids were stained with 4′,6-diamidino-2-phenylindole (Sigma) and observed for GFP and 4′,6-diamidino-2-phenylindole using fluorescence microscopy (Olympus, Tokyo, Japan). HepG2 cells were co-transfected with reporter plasmids (0.25 μg) and expression plasmids (0.75 μg) using Lipofectamine 2000 (Invitrogen, Beijing, China). Luciferase assays were performed using the Dual-Luciferase Reporter Assay System (Promega).[17]

Chromatin Immunoprecipitation Assays

Chromatin immunoprecipitation (ChIP) assays were performed with ZHX2-HA (pcZHX2)-transfected HepG2 cells. Briefly, transfected cells were fixed in 1% formaldehyde after 48 hours and sonicated to shear DNA to 200~1000 bp. Supernatants obtained after centrifugation at 13,000×g for 10 minutes were used for immunoprecipitations using an anti-HA antibody (ab9110; Abcam) or control IgG. Immunoprecipitated DNA was used for PCR amplification. Total cellular DNA was used as input control.

Patient Samples and Immunohistochemical Staining

Eighty-two tumor tissues and 78 adjacent nontumor tissues were collected from patients with primary HCC who underwent surgery between October 30, 2010, and August 31, 2011, at Qilu Hospital and Shandong Provincial Hospital, Shandong University (Supplementary Table 3). Cell differentiation-

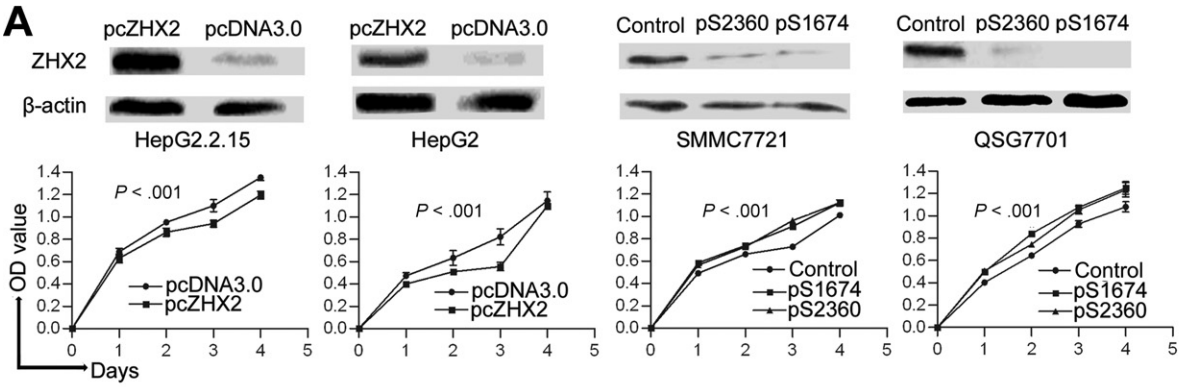
A
pcZHX2
pcDNA3.0
ZHX2
β-actin
HepG2.2.15
HepG2
Control
pS2360
pS1674
SMMC7721
QSG7701
OD value
Days
P < .001
pcDNA3.0
pcZHX2
Control
pS1674
pS2360

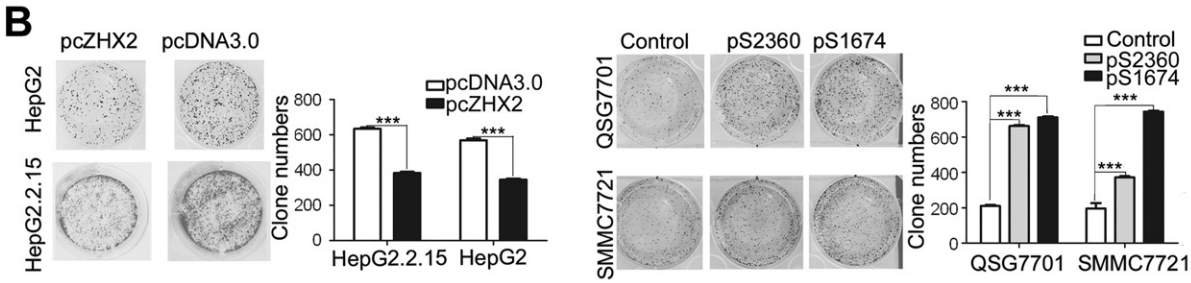
B
pcZHX2
pcDNA3.0
HepG2
HepG2.2.15
Clone numbers
HepG2.2.15
HepG2
Control
pS2360
pS1674
QSG7701
SMMC7721

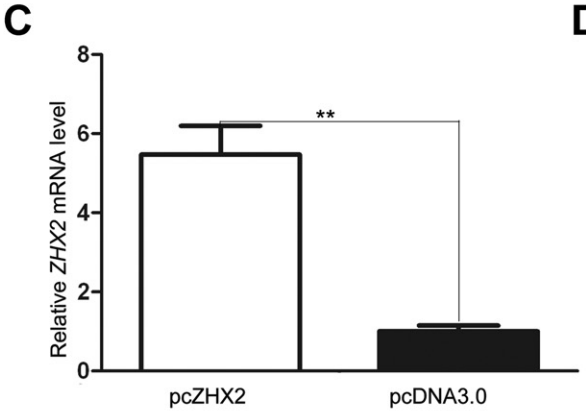
C
Relative ZHX2 mRNA level
pcZHX2
pcDNA3.0

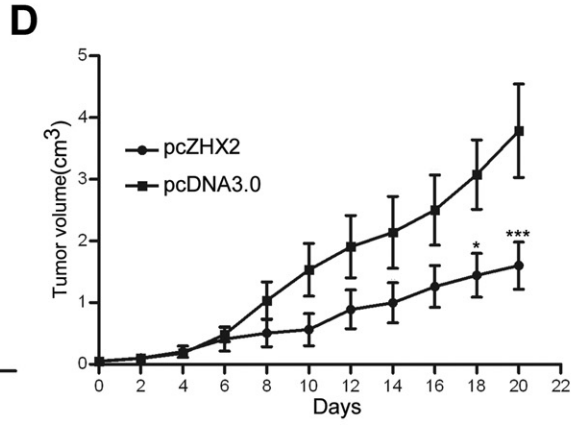
D
Tumor volume(cm3)
pcZHX2
pcDNA3.0
Days

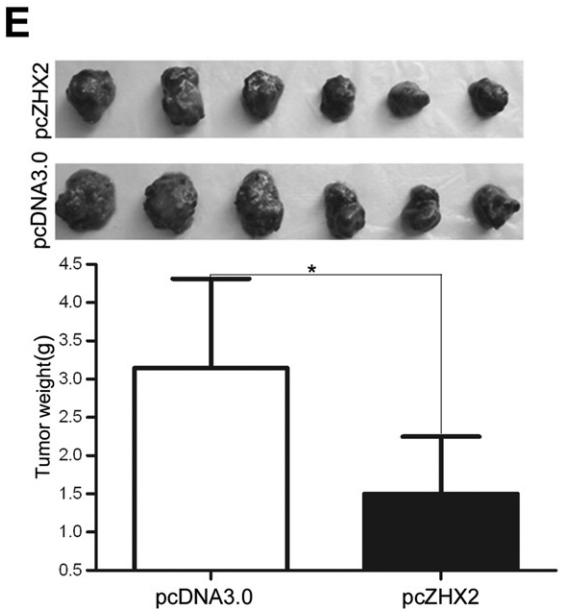
E
pcZHX2
pcDNA3.0
Tumor weight(g)
pcDNA3.0
pcZHX2

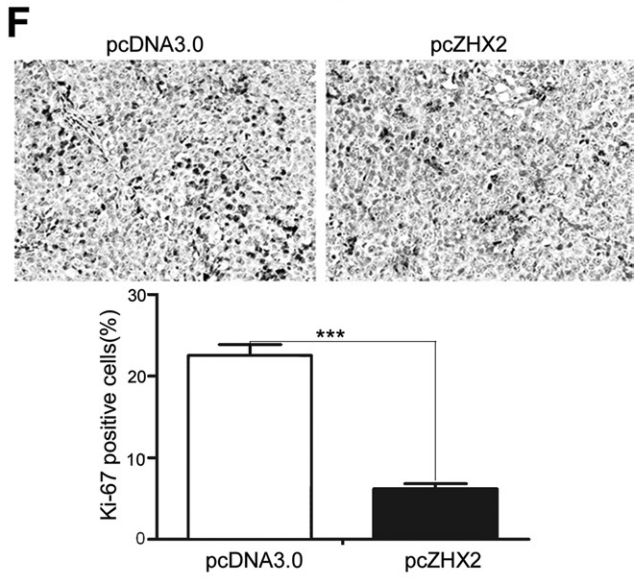
F
pcDNA3.0
pcZHX2
Ki-67 positive cells(%)
pcDNA3.0
pcZHX2

based HCC tumor grading was determined as described by Edmondson and Steiner.[23] Liver fibrosis was staged using the Ishak score and samples with a score more than 5 were classified as cirrhotic.[24] The presence of hepatitis B virus antigens was determined by enzyme-linked immunosorbent assay. None of the patients were positive for hepatitis C virus or human immunodeficiency virus, consumed excessive alcohol, or received chemotherapy before surgery. Informed consent was obtained from all patients before the study was initiated with approval of the Shandong University Medical Ethics Committee in accordance with the Declaration of Helsinki. Tissue microarrays were purchased from the Shanghai Outdo Biotech Company (Shanghai, China).

Immunohistochemical staining was performed according to standard protocols using the following antibodies: anti-ZHX2 (ab56886; Abcam), anti–Ki-67 (ab15580; Abcam), anti–Cyclin A (#4656; Cell Signaling Technology), anti–Cyclin E (sc-25303; Santa Cruz Biotechnology), and anti-CD31 (#3528; Cell Signaling Technology). Eight fields of approximately 1000 cells from each tumor and nontumor sections were counted independently by 3 pathologists. Cytoplasmic and nuclear ZHX2 staining were reported separately according to the German semiquantitative scoring system.[25,26] Briefly, each sample was scored according to staining intensity (no staining = 0; weak staining = 1; moderate staining = 2; and strong staining = 3) and the number of stained cells (0% = 0; 1%–25% = 1; 26%–50% = 2; 51%–75% = 3; and 76%–100% = 4). Final immunoreactive scores were determined by multiplying the staining intensity by the number of stained cells, with minimum and maximum scores of 0 and 12, respectively.[27] Levels of hepatocyte proliferation and intratumoral microvascular density (MVD) were identified by Ki-67 and CD31 staining, respectively. For quantization of MVD, the average numbers of CD31-positive vessels from 3 areas of maximal vascular density (vascular hotspots) were counted for each section.[28]

Statistical Analysis

GraphPad Prism (GraphPad Software, San Diego, CA) was used for data analysis. The Student *t* test, Mann–Whitney *U* test, or one-way analysis of variance (ANOVA) was applied to determine significant differences between groups. Two-way ANOVA was applied to determine significant differences between different treatments, in different cell cohorts, or at different time points. The statistical correlation between the clinical parameters of HCC and the ZHX2 staining levels in tissue sections was analyzed by the chi-square test. Survival differences were analyzed using the log-rank test. In these analyses, *P* values less than .05 were considered significant.

Results

ZHX2 Inhibited the Proliferation of HCC Cell Lines Both In Vitro and In Vivo

Previous studies provided conflicting data regarding a potential role for ZHX2 in HCC progression. To investigate further the role of ZHX2 in hepatocarcinogenesis, we measured the growth of hepatoma cell lines in which ZHX2 levels were modulated. The HCC cell lines HepG2 and HepG2.2.15 have low endogenous ZHX2 levels. In both cell lines, ZHX2 overexpression reduced proliferation over a 4-day period (Figure 1*A*). Consistent with these data, reducing ZHX2 levels by transfecting shRNAs pS1674 and pS2360 in HCC cell lines SMMC7721 and QSG7701, which have high endogenous ZHX2 levels, significantly enhanced cell proliferation (Figure 1*A*). The inhibitory properties of ZHX2 also were analyzed using colony formation assay. ZHX2 overexpression led to a significant decrease in the number of colonies formed when assayed 10 days after transfection in both HepG2 and HepG2.2.15 cell lines (Figure 1*B*). The shRNA-mediated knockdown of ZHX2 significantly increased the number of colonies formed in both the QSG7701 and SMMC7721 cell lines (Figure 1*B*). Taken together, these results indicate that ZHX2 inhibits the proliferation of HCC cell lines.

The influence of ZHX2 on tumor growth was evaluated further by measuring growth of subcutaneous HepG2.2.15 xenografts in nude mice. After reaching a diameter of 0.5 cm, tumors were injected with pcDNA3.0 or pcZHX2. Real-time reverse-transcription PCR analysis showed that pcZHX2-injected tumors had increased ZHX2 messenger RNA (mRNA) levels compared with pcDNA3.0-injected tumors (Figure 1*C*). Moreover, injection of pcZHX2 significantly inhibited the tumor growth over the course of the experiment (Figure 1*D*). Consistent with this finding, the weight of ZHX2-injected tumors at the time of death was less than half of pcDNA3.0-injected control tumors (Figure 1*E*).

Immunohistochemical analysis showed less Ki-67 staining in pcZHX2-treated tumors (Figure 1*F*), indicative of reduced proliferation. Taken together, these in vitro and in vivo studies indicate that ZHX2 inhibits cell growth and, consistent with ZHX2, functioning as a tumor suppressor.

Figure 1. Increased ZHX2 levels inhibit growth of HCC both (*A* and *B*) in vitro and (*C–F*) in vivo. (*A*) Proliferation of HepG2.2.15 and HepG2 cells transfected with pcZHX2 or control pcDNA3.0 and SMMC7721 and QS7701 cells transfected with shRNAs pS2360 or pS1674. Cells were assayed over a 4-day period, and data shown are mean ± SD from 4 experiments. ZHX2 and β-actin levels in cell lines were determined by Western blot. (*B*) Colony formation of HCC cell lines transfected with pcZHX2 or ZHX2 shRNAs were as described in *panel A*. Plates are shown on the *left*; the statistical results are shown on the *right* (mean ± SD from 3 experiments). ***$P < .001$. (*C*) Real-time reverse-transcription PCR analysis of *ZHX2* mRNA in pcZHX2-injected tumors and control pcDNA3.0-injected tumors (mean ± SD, n = 6). **$P < .01$. (*D*) Xenograft tumor growth determined over a 20-day period (mean ± SD, n = 6). *$P < .05$, ***$P < .001$. (*E*) Weight of pcZHX2- and pcDNA3.0-injected tumors at time of death (mean ± SD, n = 6). *$P < .05$. Images of tumors from each group are shown on *top*. (*F*) Immunohistochemical staining of Ki-67 of pcDNA3.0- and pcZHX2-injected tumors; statistical results are shown on the *bottom* (mean ± SD, n = 6). ***$P < .001$.

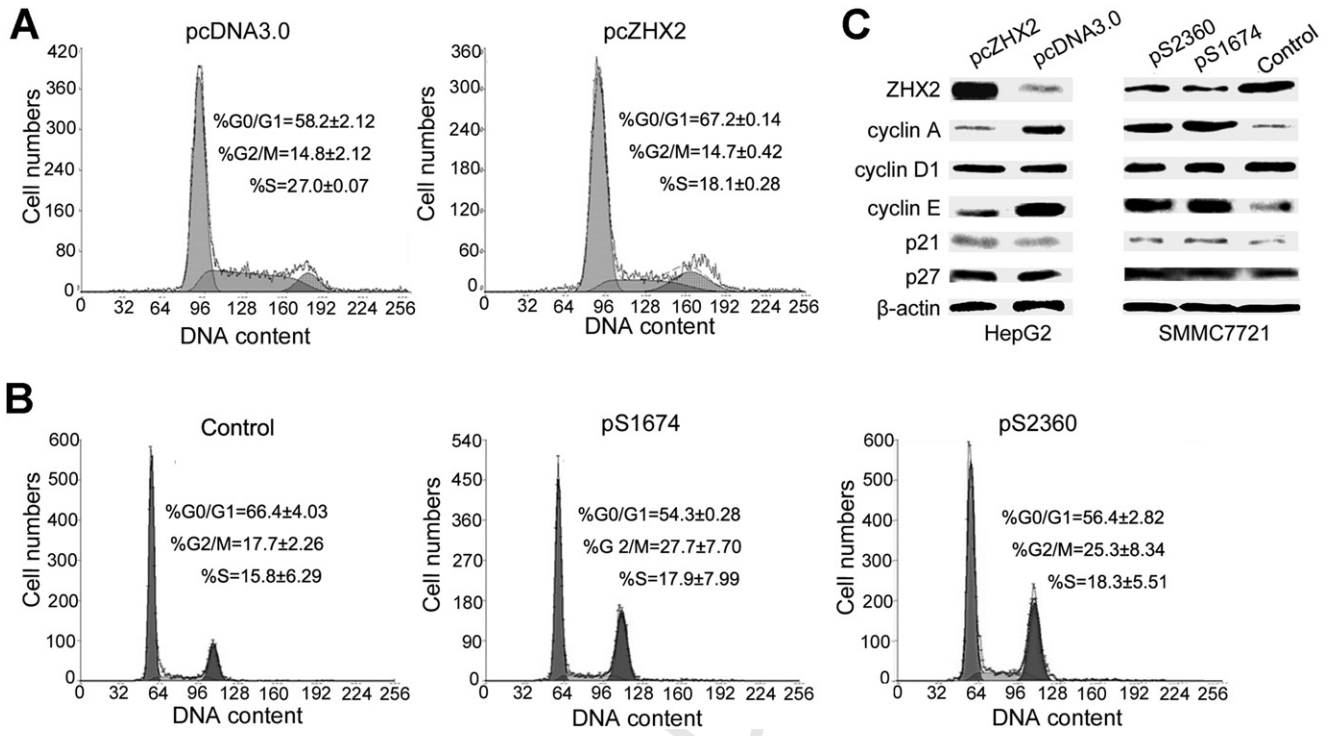

Figure 2. ZHX2 induces G1 arrest and represses Cyclin A and Cyclin E expression. (*A*) HepG2 cells transfected with pcZHX2 or pcDNA3.0 or (*B*) SMMC7721 cells transfected with scrambled control vector or pS1764 or pS2360 shRNA vectors were analyzed by propidium iodide staining and flow cytometry. A representative plot from one experiment and mean ± SD from 3 experiments are shown. (*C*) Western blot to monitor levels of ZHX2, Cyclin A, Cyclin D1, Cyclin E, p21, p27, and β-actin in transfected HCC cell lines described in *panels A* and *B*. The experiments were repeated 4 times, and one representative result is shown.

ZHX2 Induces G1 Arrest and Represses Cyclin A and Cyclin E Expression

To explore the mechanism by which ZHX2 inhibits cell growth, cell-cycle analysis was performed by propidium iodide staining and flow cytometry of HCC cell lines in which ZHX2 levels were increased or decreased. F2 Transfection of pcZHX2 in HepG2 cells (Figure 2*A*) and HepG2.2.15 cells (data not shown) increased the percentage of G0/G1 cells and decreased the percentage of S-phase cells. In a reciprocal experiment, shRNA-mediated reduction of ZHX2 in SMMC7721(Figure 2*B*) and QSG7701 cells (data not shown) by pS1674 or pS2360 decreased and increased the percentage of cells in G0/G1 and G2/M, respectively. Analysis of potential cell-cycle regulators indicated that ZHX2 overexpression in HepG2 cells decreased Cyclin A and Cyclin E but had no effect on Cyclin D1, p21, or p27 protein levels (Figure 2*C*). The shRNA-mediated reduction of ZHX2 in SMMC7721 cells led to increased Cyclin A and Cyclin E levels whereas Cyclin D1, p21, and p27 levels remained unchanged (Figure 2*C*). These data suggest that ZHX2 influences cell-cycle progression by reducing Cyclin A and/or Cyclin E levels.

ZHX2 Inhibits Cell Proliferation by Reducing Cyclin A and Cyclin E Transcription

Previous studies have suggested that ZHX2 functions as a transcriptional repressor.[14] Because our Western data indicated that Cyclin A and Cyclin E levels inversely correlated with ZHX2 levels, we considered whether ZHX2 represses the transcription of these genes. Real-time reverse-transcription PCR analysis showed that Cyclin A and Cyclin E steady-state mRNA levels were decreased dramatically when ZHX2 levels were increased in HepG2 cells and increased when ZHX2 levels were reduced in SMMC7721 cells (Figure 3*A*). To explore this regulation F3 further, the Cyclin A and Cyclin E promoters were fused to a luciferase reporter gene (Figure 3*C*). Transient co-transfections showed that ZHX2 repressed the activities of both promoters (Figure 3*B*). To determine if this regulation involved ZHX2 binding to these promoters, ChIP assays were performed in HepG2 cells transfected with HA-tagged ZHX2. These data indicated that ZHX2 binds the promoter regions of both Cyclin A and Cyclin E but not Cyclin D1 (Figure 3*D*), suggesting that ZHX2 represses Cyclin A and Cyclin E expression by binding, directly or indirectly, to the promoters of these genes.

The growth inhibitory properties of ZHX2 may be owing to its ability to repress Cyclin A and Cyclin E. If so, reducing these cyclins should overcome the effects of reducing ZHX2 levels. To test this possibility, Cyclin A and Cyclin E protein levels were reduced by siRNAs in the same cells where ZHX2 levels were knocked down. Indeed, we found that the siRNAs against these cyclins abrogated the accelerated growth mediated by the ZHX2 shRNAs in SMMC7721 or QSG7701 cells in both colony growth and cell proliferation assays (Figures 3*E* and *F*). In contrast,

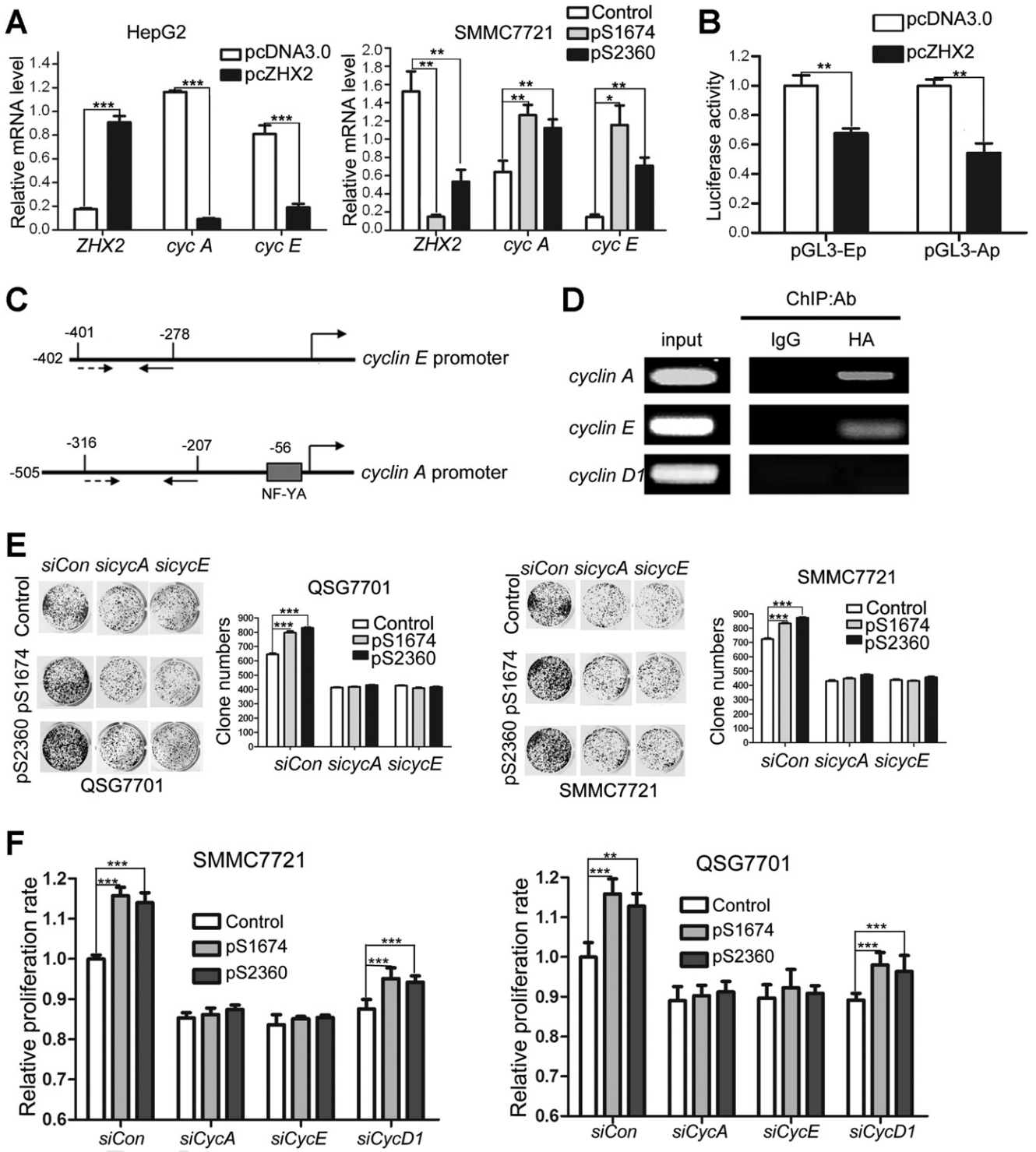

Figure 3. ZHX2 binds to and represses activity of the Cyclin A and Cyclin E promoters. (*A*) Real-time reverse-transcription PCR analysis of ZHX2, Cyclin A, and Cyclin E mRNA levels in HepG2 cells transfected with pcZHX2 or pcDNA3.0 or SMMC7721 cells transfected with shRNAs. Data (mean ± SD) of 3 experiments are shown. *$P < .05$, **$P < .01$, ***$P < .001$. (*B*) Inhibition of the pGL3-Ep and pGL3-Ap luciferase reporter genes by ZHX2 in HepG2 cells. Data (mean ± standard error of the mean) of 4 experiments are shown. **$P < .01$. (*C*) Diagram of the Cyclin E and Cyclin A promoters, extending to −402 and −505, respectively, including the NF-Y site in the Cyclin A promoter[34] and location of the primers (*solid or dotted lines* under promoters) used for ChIP analysis. (*D*) ChIP analysis of DNA from HepG2 cells transfected with ZHX2-HA. PCR amplification of HA-immunoprecipitated DNA using the primers shown in *panel C* shows ZHX2 binding to Cycln A and Cyclin E promoters but not Cyclin D1. One of 3 independent experiments is shown. (*E*) Colony formation of QSG7701 and SMMC7721 cells transfected with shRNAs against ZHX2 (pS1674 or pS2360) and siRNAs against Cyclin A (*sicycA*) or Cyclin E (*sicyc*E). One representative plate of each group is shown on the *left*; results from 3 independent experiments are shown on the *right* (mean ± SD). ***$P < .001$. (*F*) Proliferation of QSG7701 and SMMC7721 cells that were co-transfected with ZHX2 shRNAs along with siRNAs for Cyclin A, Cyclin E, or Cyclin D1. Cells were measured using CCK-8 at 48 hours after cotransfection. Mean ± SD of 3 experiments is shown. **$P < .01$; ***$P < .001$.

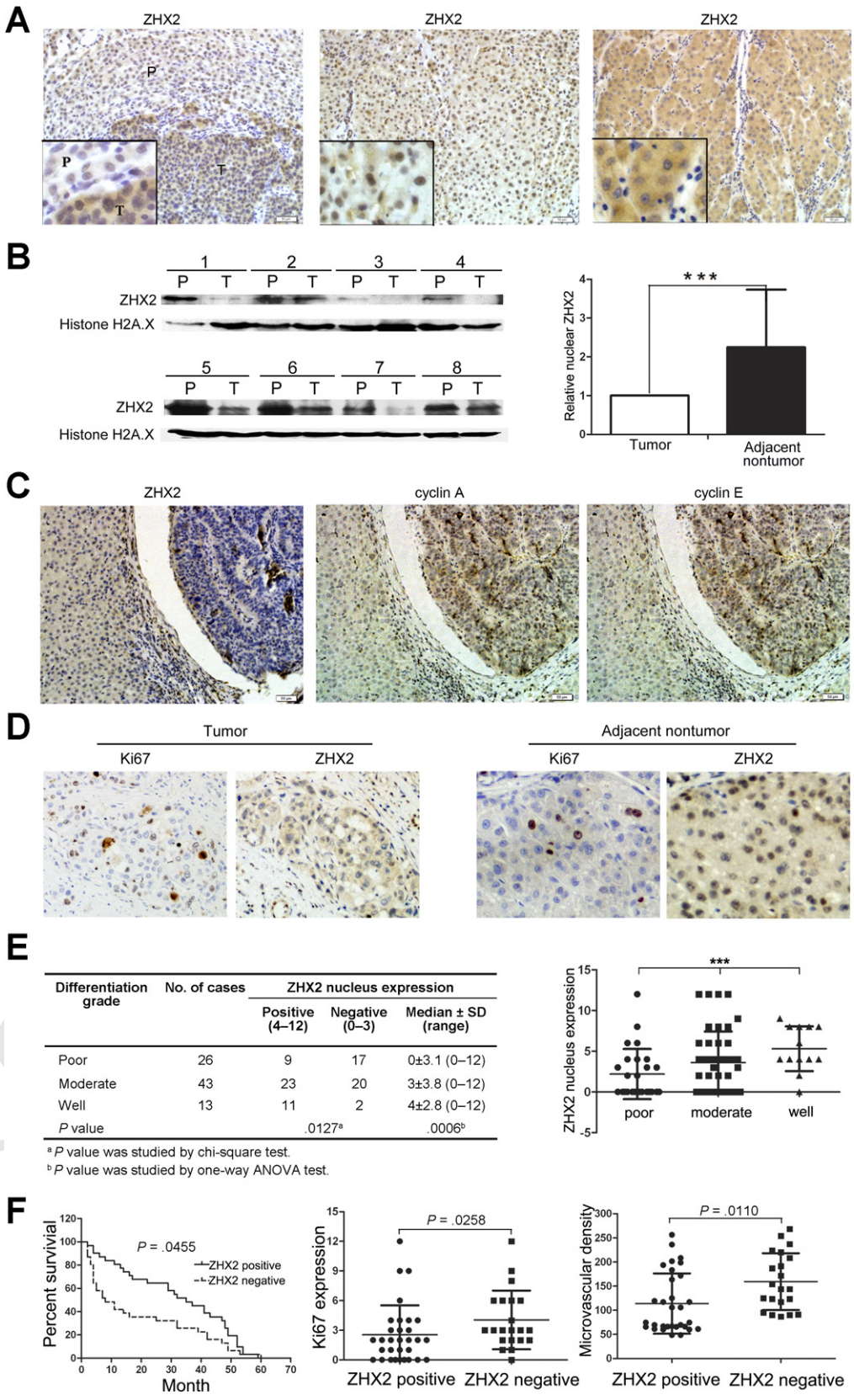

E

Differentiation grade	No. of cases	ZHX2 nucleus expression		
		Positive (4–12)	Negative (0–3)	Median ± SD (range)
Poor	26	9	17	0±3.1 (0–12)
Moderate	43	23	20	3±3.8 (0–12)
Well	13	11	2	4±2.8 (0–12)
P value		.0127[a]		.0006[b]

[a] *P* value was studied by chi-square test.
[b] *P* value was studied by one-way ANOVA test.

Figure 4. ZHX2 expression in HCC and correlation with clinical parameters. (*A*) Immunohistochemical staining of ZHX2 in HCC sections (*left* and *right*) and nontumor liver sections (*middle*). T, tumor; P, adjacent nontumor. Original magnification, 200×. (*B*) Western blot analysis of ZHX2 levels in nuclear extracts of adjacent nontumor (P) and tumor (T) samples from patients with HCC. Histone H2A.X was used as a control. Statistical data are shown (*right*). ***$P < .001$. (*C*) Immunohistochemical staining of ZHX2 (*left*), Cyclin A (*middle*), and Cyclin E (*right*) in adjacent sections of a cancer biopsy from 1 patient. Original magnification, 200×. (*D*) Immunohistochemical staining of ZHX2 and Ki-67 (marker of cell proliferation) in continuous biopsy specimens (tumor sections and adjacent nontumor sections). (*E*) Statistical analysis of ZHX2 nuclear expression in poor, moderate, or highly differentiated HCC samples. The immunoreactive score is shown as median ± SD. ***$P < .001$. (*F*) Nuclear ZHX2 expression correlates with overall survival (*left*), Ki-67 (*middle*), and intratumoral microvascular density (*right*).

COLOR

AQ: 31

the increased proliferation of cells treated with shRNAs against ZHX2 was not overcome by reducing Cyclin D1 levels (Figure 3*F*). These data support the possibility that ZHX2 inhibits HCC cell growth, at least in part, by inhibiting Cyclin A and Cyclin E expression.

Nuclear but Not Cytoplasmic ZHX2 Expression Is Decreased in HCC Tissues

Previous studies provided conflicting data regarding ZHX2 expression in HCC.[20] To explore ZHX2 expres-

sion in liver cancer further, we stained for ZHX2 in both HCC and adjacent nontumor regions (Figure 4*A*). ZHX2 staining was observed in both regions. However, the percentage of positive nuclear staining (score, 4–12) was significantly higher in adjacent nontumor regions compared with that in tumors ($P = .0282$; Table 1). In contrast, the percentage of positive cytoplasmic ZHX2 staining in tumors was significantly higher than that in adjacent nontumor sections ($P = .0190$; Table 1). Overall, there was no difference in total ZHX2 expression (nuclear and cytoplasmic staining) between tumor and adjacent nontumor groups (Table 1). This difference in nuclear/cytoplasmic ZHX2 staining is supported by Western blot analysis of nuclear extracts from tumors and adjacent nontumor tissue, with nuclear ZHX2 being lower in tumor nuclei (Figure 4*B*). Interestingly, decreased nuclear ZHX2 staining also was observed in tumors with diameters less than 5 cm (Table 1).

Consistent with our in vitro data with HCC cell lines, we found that decreased nuclear ZHX2 expression was accompanied by increased expression of Cyclin A and Cyclin E in continuous tissue sections from the same patients (Figure 4*C*), suggesting the inhibitory effect of ZHX2 on cell proliferation in vivo. In addition, less nuclear ZHX2 expression correlated with greater Ki-67+ nuclei in HCC sections (Figure 4*D*). Moreover, ZHX2 nuclear expression was significantly higher in well-differentiated tumor tissues (84.6%) than that in moderately (53.5%) or poorly differentiated (34.6%) tumor tissues (Figure 4*E*; $P = .0006$), suggesting a correlation of nuclear ZHX2 with HCC progression. To further test this, tissue arrays containing 106 cores were analyzed for ZHX2 expression (Supplementary Figure 1). Reduced nuclear ZHX2 expression was observed in liver cancer samples, including specimens from small tumors (diameter, ≤5 cm). In addition, decreased nuclear staining of ZHX2 significantly correlated with reduced overall survival times of patients. Consistently, levels of hepatocyte proliferation (Ki-67 as the marker) and intratumoral MVD (CD31 as the marker) were significantly higher in tissues without nuclear ZHX2 expression compared with that with higher ZHX2 expression (Figure 4*F*). Taken together, our data show that reduced nuclear ZHX2 levels correlate with HCC progression and that this reduction likely occurs at an early stage of liver cancer.

Nuclear ZHX2 Localization Is Essential for Inhibition of Cell Proliferation

Our data showing decreased nuclear ZHX2 levels in HCC tissues (Figure 4 and Table 1) led us to hypothesize that ZHX2 must localize to the nucleus to inhibit cell growth. To directly test this possibility, we generated ZHX2–EGFP fusion proteins, including full-length ZHX2 (pZHX2), pZHX2(242–446), which contains the ZHX2 dimerization domain and NLS, and pZHX2(242–439), which contains the dimerization domain without the NLS. Constructs were transfected transiently into 293 cells and CHO cells. By both fluorescence staining and Western blot with cytoplasmic and nuclear extracts, we

Table 1. Detection of ZHX2 Expression in Clinical Specimens

		ZHX2 expression									
		Nuclear staining			Cytoplasmic staining			Nuclear plus cytoplasmic staining			
	Cases, n	Positive (4–12)	Negative (0–3)	Median ± SD (range)	Positive (4–12)	Negative (0–3)	Median ± SD (range)	Positive (4–12)	Negative (0–3)	Median ± SD (range)
All specimens											
Cancer	82	44 (53.7%)	38 (46.3%)	4 ± 1.2 (0–12)	39 (47.6%)	43 (52.4%)	3 ± 3.5 (0–12)	37 (45.1%)	45 (54.9%)	3 ± 3.4 (0–12)
Noncancer	78	55 (70.5%)	23 (29.5%)	4 ± 4.1 (0–12)	23 (29.5%)	55 (70.5%)	0 ± 2.1 (0–8)	35 (44.9%)	43 (55.1%)	3 ± 2.7 (0–10)
P value		.0282[a]		.0523[b]	.0190[a]		.0011[b]	.97641[a]		.8351[b]
Specimens with small tumor (≤5 cm)											
Cancer	51	25 (49%)	26 (51%)	3.5 ± 4.1 (0–12)	21 (41.2%)	30 (58.8%)	3 ± 3.5 (0–12)	19 (37.3%)	32 (62.7%)	3.2 ± 3.1 (0–12)
Noncancer	48	33 (68.8%)	15 (31.2%)	5.1 ± 3.7 (0–12)	10 (20.8%)	38 (79.2%)	1.2 ± 1.7 (0–4)	18 (37.5%)	30 (62.5%)	3.1 ± 2.4 (0–8)
P value		.0464[a]		.0428[b]	.0292[a]		.0017[b]	.9799[a]		.8876[b]

[a]*P* values were obtained from the chi-square test.
[b]*P* values were obtained from the nonparametric test.

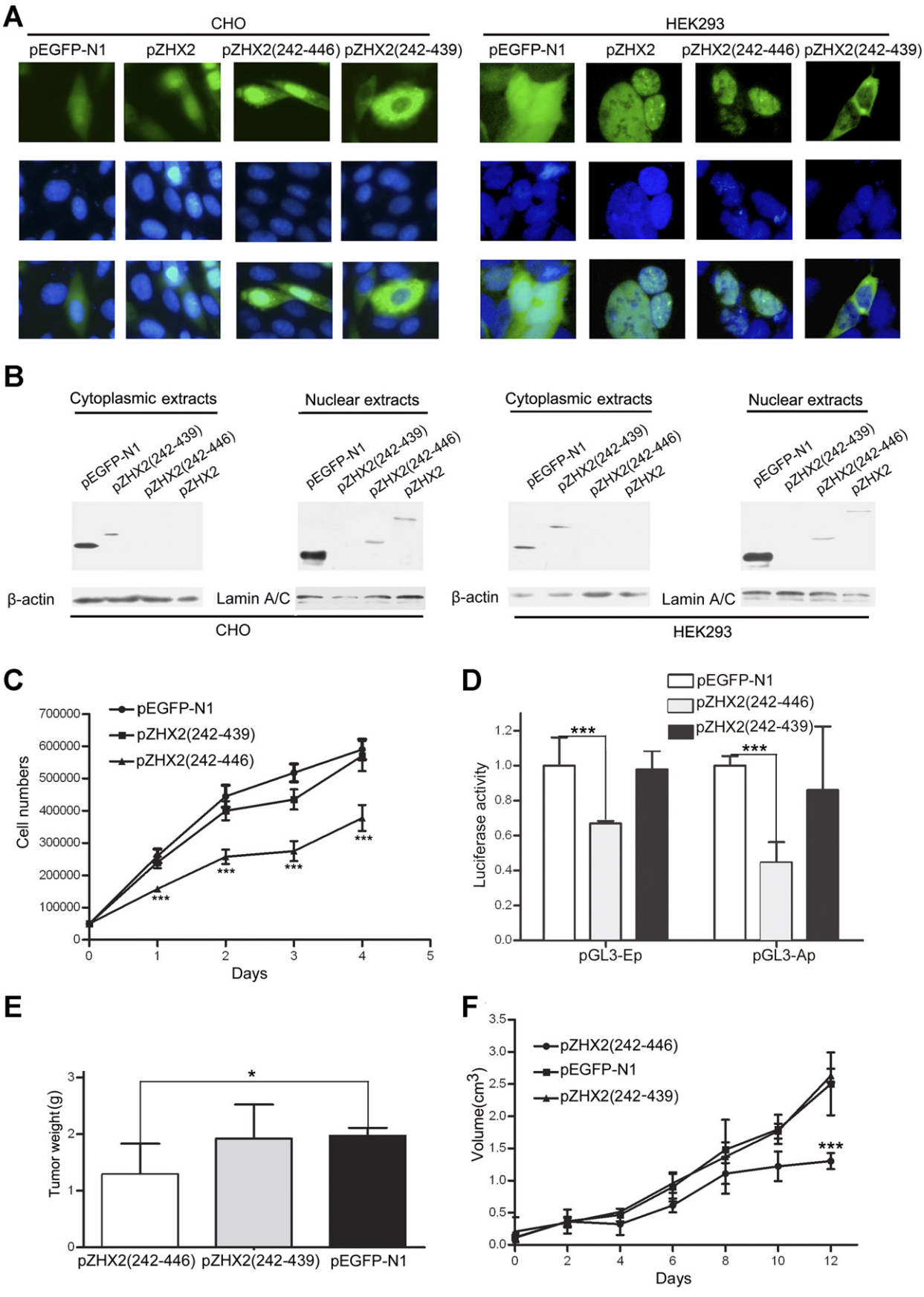
A
CHO
HEK293
pEGFP-N1
pZHX2
pZHX2(242-446)
pZHX2(242-439)
B
Cytoplasmic extracts
Nuclear extracts
pEGFP-N1
pZHX2(242-439)
pZHX2(242-446)
pZHX2
β-actin
Lamin A/C
CHO
HEK293
C
pEGFP-N1
pZHX2(242-439)
pZHX2(242-446)
Cell numbers
Days
D
pEGFP-N1
pZHX2(242-446)
pZHX2(242-439)
Luciferase activity
pGL3-Ep
pGL3-Ap
E
Tumor weight(g)
pZHX2(242-446)
pZHX2(242-439)
pEGFP-N1
F
pZHX2(242-446)
pEGFP-N1
pZHX2(242-439)
Volume(cm3)
Days

found that EGFP fusion proteins with full-length ZHX2 and ZHX2(242–446) were localized mainly to the nucleus, whereas ZHX2(242–439) and the control pEGFP-N1 were found predominantly in the cytoplasm (Figure 5*A* and *B*). In addition, pZHX2(242–446), but not ZHX2(242–439), inhibited the proliferation of HepG2 cells (Figure 5*C*) and activity of pGL3-Ep and pGL3-Ap reporter constructs (Figure 5*D*). Moreover, injection of ZHX2(242–446) but not ZHX2(242–439) inhibited the weight (Figure 5*E*) and growth (Figure 5*F*) of HepG2.215 tumors in our xenograft model. Collectively, these data indicate that nuclear ZHX2 localization is essential for its ability to inhibit cell growth in vitro and in vivo.

Discussion

ZHX2 has been described as a transcriptional repressor, possibly through its interactions with NF-YA.[14] Based on changes in its expression, ZHX2 has been implicated in several human diseases, including podocyte disease and multiple myeloma.[29,30] Conflicting data exist regarding ZHX2 in HCC.[19,20] Here, we show that nuclear ZHX2 levels are reduced in HCC, including small tumors (diameter, ≤5 cm), suggesting that the loss of nuclear ZHX2 is an early event in HCC progression. Moreover, we show that ZHX2 significantly inhibits the growth of HCC cell lines in vitro and in vivo. Analysis of clinical HCC samples showed a significant correlation between reduced nuclear ZHX2 and poor overall survival as well as increased levels of microvascularization and hepatocyte proliferation. Finally, studies in BALB/cJ mice indicate that ZHX2 is a negative regulator of the tumor markers AFP, GPC3, and H19 in the adult liver.[9,10] Taken together, these data suggest that ZHX2 functions to suppress HCC growth and is consistent with the previous report that identified hypermethylation in the *ZHX2* promoter, along with silencing of ZHX2 expression, in HCC tissues.[19]

One important question is how ZHX2 inhibits the growth of HCC cell lines. Our data suggests that this may occur through its transcriptional repression of Cyclin A and Cyclin E, both of which are key cell-cycle regulators. Cyclin A is associated with CDK2 and responsible for the control of S-phase progression and the G2-M transition.[31] Ectopic Cyclin E overexpression can accelerate cell-cycle progression from the G1 to S phase and reinforce the loss of growth control.[32] A previous report showed ZHX2-mediated repression of the proliferation-related gene *cdc25C*.[14] Because Cyclin A, Cyclin E, and cdc25C function in many cells and ZHX2 is expressed ubiquitously, we hypothesize that the growth inhibitory effect of ZHX2 would not be restricted to HCC but could act in multiple cell types. This possibility is supported by a recent report suggesting that the loss of *ZHX2* expression confer to myeloma cells a stem cell–like phenotype resulting in a resistance to chemotherapy.[33] Therefore, identification of novel genes regulated by *ZHX2* not only will provide insight into tumorigenesis but also provide new targets for tumor therapy and diagnosis.

By using luciferase reporter genes, we show that ZHX2 controls the Cyclin A and Cyclin E promoters. This is consistent with a recent report by Gargalovic et al,[11] which reported increased hepatic Cyclin E expression in BALB/cJ mice, which have a mutated *ZHX2* gene. Our ChIP data indicate that ZHX2 can bind the Cyclin A and Cyclin E promoters and we show ZHX2 binding to a target promoter. ZHX2, similar to other ZHX proteins, is thought to regulate at least some target genes in a NF-Y–dependent manner.[14,18] NF-YA binds to the CCAAT element at −52 of the *Cyclin A* promoter.[34,35] Whether NF-Y or the CCAAT element in the Cyclin A promoter is required for ZHX2-mediated repression is not known. Also, there is no evidence of NF-YA binding to the promoters of the *Cyclin E* or *AFP* genes. Although ZHX2 is considered to function at the transcriptional level,[14,17] there is evidence that it also acts post-transcriptionally.[9,36,37] Understanding this aspect of ZHX2-mediated regulation will require further study.

Previous studies localized the NLS of ZHX2 to amino acids 317–446.[14] By using EGFP fusion proteins, our data indicate that ZHX2(242–446) is localized to the nucleus whereas ZHX2(242–439) remains cytoplasmic. The cytoplasmic form of ZHX2 no longer inhibited Cyclin A and Cyclin E promoters or reduced cell proliferation in HCC cell lines or tumor growth in nude mice, whereas the nuclear form ZHX2(242–446) retained these functions. These data indicate that nuclear location of ZHX2 is required for its growth-inhibitory properties. This is consistent with our analysis of clinical samples, in which we detected decreased nuclear ZHX2 expression at the level of protein but not total ZHX2 protein (Table 1) and mRNA (Supplementary Figure 1) in HCC compared with nontumor tissues. This might account for the failure to identify ZHX2 as an HCC relevant gene by transcriptome analysis.[38] The loss of nuclear localization might occur during the early stages of tumorigenesis because this was observed in small liver tumors (diameter, ≤5 cm). This change of ZHX2 expression pattern might be, at least partially, responsible for increased proliferation and tu-

Figure 5. Nuclear ZHX2 localization is essential for growth inhibition in vitro and in vivo. CHO and 293 cells were transfected transiently with pZHX2(242–446), pZHX2(242–439), full-length pZHX2, and pEGFP-N1. (*A*) ZHX2 localization was determined by fluorescence microscopy of EGFP. DAPI (*blue*) was used to stain nuclei. Original magnification, 200×. (*B*) Western blot analysis of EGFP and EGFP fusion proteins in cytoplasm and nuclei. (*C*) Proliferation of HepG2 for 4 days after transfection with pZHX2(242–439), pZHX2(242–446), and pEGFP-N1. ***$P < .001$. (*D*) Activity of the pGL3-Ep and pGL3-Ap in HepG2 cells co-transfected with pZHX2(242–439), pZHX2(242–446), and pEGFP-N1. Data shown are mean ± SD of 3 independent experiments. ***$P < .001$. (*E* and *F*) Tumors of HepG2.2.15 cells grown in nude mice were injected with pZHX2(242–439), pZHX2(242–446), or pEGFP-N1. (*E*) Weights of tumors were determined after death (mean ± SD; n = 6). *$P < .05$. (*F*) Tumor volume was calculated every other day over 12 days (mean ± SD; n = 6). ***$P < .001$.

COLOR

mor development. This is supported by the correlation of nuclear ZHX2 level with HCC progression markers, including disease grade of liver cancer, patients' overall survival, and levels of tumor microvascularization and hepatocyte proliferation, detected in HCC tissues.

In conclusion, our study indicates that ZHX2 controls cell proliferation in a manner that may involve regulation of cyclin A and cyclin E expression. These data provide new insight into the mechanisms by which ZHX2 might function as a tumor suppressor in liver cancer. Also, these studies with truncated forms of ZHX2 indicate that homeodomains 1 and 2 are sufficient for the growth-inhibitory properties of ZHX2. Further studies will be required to investigate the function of other domains of ZHX2, including 2 zinc fingers and 2 additional homeodomains.

Supplementary Material

Note: To access the supplementary material accompanying this article, visit the online version of *Gastroenterology* at www.gastrojournal.org, and at http://dx.doi.org/10.1053/j.gastro.2012.02.049.

References

1. Bosch FX, Ribes J, Diaz M, et al. Primary liver cancer: worldwide incidence and trends. Gastroenterology 2004;127:S5–S16.
2. El-Serag HB, Mason AC. Risk factors for the rising rates of primary liver cancer in the United States. Arch Intern Med 2000;160:3227–3230.
3. Dragani TA. Risk of HCC: genetic heterogeneity and complex genetics. J Hepatol 2010;52:252–257.
4. Peterson ML, Ma C, Spear BT. Zhx2 and Zbtb20: novel regulators of postnatal alpha-fetoprotein repression and their potential role in gene reactivation during liver cancer. Semin Cancer Biol 2011;21:21–27.
5. Abelev GI. Alpha-fetoprotein in ontogenesis and its association with malignant tumors. Adv Cancer Res 1971;14:295–358.
6. Wang XY, Degos F, Dubois S, et al. Glypican-3 expression in hepatocellular tumors: diagnostic value for preneoplastic lesions and hepatocellular carcinomas. Hum Pathol 2006;37:1435–1441.
7. Ariel I, Miao HQ, Ji XR, et al. Imprinted H19 oncofetal RNA is a candidate tumour marker for hepatocellular carcinoma. Mol Pathol 1998;51:21–25.
8. Abelev GI, Eraiser TL. Cellular aspects of alpha-fetoprotein reexpression in tumors. Semin Cancer Biol 1999;9:95–107.
9. Spear BT, Jin L, Ramasamy S, et al. Transcriptional control in the mammalian liver: liver development, perinatal repression, and zonal gene regulation. Cell Mol Life Sci 2006;63:2922–2938.
10. Perincheri S, Dingle RW, Peterson ML, et al. Hereditary persistence of alpha-fetoprotein and H19 expression in liver of BALB/cJ mice is due to a retrovirus insertion in the Zhx2 gene. Proc Natl Acad Sci U S A 2005;102:396–401.
11. Gargalovic PS, Erbilgin A, Kohannim O, et al. Quantitative trait locus mapping and identification of Zhx2 as a novel regulator of plasma lipid metabolism. Circ Cardiovasc Genet 2010;3:60–67.
12. Barthelemy I, Carramolino L, Gutierrez J, et al. zhx-1: a novel mouse homeodomain protein containing two zinc-fingers and five homeodomains. Biochem Biophys Res Commun 1996;224:870–876.
13. Kawata H, Yamada K, Shou Z, et al. The mouse zinc-fingers and homeoboxes (ZHX) family; ZHX2 forms a heterodimer with ZHX3. Gene 2003;323:133–140.
14. Kawata H, Yamada K, Shou Z, et al. Zinc-fingers and homeoboxes (ZHX) 2, a novel member of the ZHX family, functions as a transcriptional repressor. Biochem J 2003;373:747–757.
15. Bird LE, Ren J, Nettleship JE, et al. Novel structural features in two ZHX homeodomains derived from a systematic study of single and multiple domains. BMC Struct Biol 2010;10:13.
16. Yamada K, Kawata H, Shou Z, et al. Analysis of zinc-fingers and homeoboxes (ZHX)-1-interacting proteins: molecular cloning and characterization of a member of the ZHX family, ZHX3. Biochem J 2003;373:167–178.
17. Shen H, Luan F, Liu H, et al. ZHX2 is a repressor of alpha-fetoprotein expression in human hepatoma cell lines. J Cell Mol Med 2008;12:2772–2780.
18. Yamada K, Ogata-Kawata H, Matsuura K, et al. ZHX2 and ZHX3 repress cancer markers in normal hepatocytes. Front Biosci 2009;14:3724–3732.
19. Lv Z, Zhang M, Bi J, et al. Promoter hypermethylation of a novel gene, ZHX2, in hepatocellular carcinoma. Am J Clin Pathol 2006;125:740–746.
20. Hu S, Zhang M, Lv Z, et al. Expression of zinc-fingers and homeoboxes 2 in hepatocellular carcinogenesis: a tissue microarray and clinicopathological analysis. Neoplasma 2007;54:207–211.
21. Henglein B, Chenivesse X, Wang J, et al. Structure and cell cycle-regulated transcription of the human cyclin A gene. Proc Natl Acad Sci U S A 1994;91:5490–5494.
22. Ohtani K, DeGregori J, Nevins JR. Regulation of the cyclin E gene by transcription factor E2F1. Proc Natl Acad Sci U S A 1995;92:12146–12150.
23. Edmondson HA, Steiner PE. Primary carcinoma of the liver: a study of 100 cases among 48,900 necropsies. Cancer 1954;7:462–503.
24. Ishak KG. Pathologic features of chronic hepatitis. A review and update. Am J Clin Pathol 2000;113:40–55.
25. Han CP, Kok LF, Wang PH, et al. Scoring of p16(INK4a) immunohistochemistry based on independent nuclear staining alone can sufficiently distinguish between endocervical and endometrial adenocarcinomas in a tissue microarray study. Mod Pathol 2009;22:797–806.
26. Kamoi S, AlJuboury MI, Akin MR, et al. Immunohistochemical staining in the distinction between primary endometrial and endocervical adenocarcinomas: another viewpoint. Int J Gynecol Pathol 2002;21:217–223.
27. Han CP, Lee MY, Tzeng SL, et al. Nuclear receptor interaction protein (NRIP) expression assay using human tissue microarray and immunohistochemistry technology confirming nuclear localization. J Exp Clin Cancer Res 2008;27:25.
28. Weidner N. Current pathologic methods for measuring intratumoral microvessel density within breast carcinoma and other solid tumors. Breast Cancer Res Treat 1995;36:169–180.
29. Armellini A, Sarasquete ME, Garcia-Sanz R, et al. Low expression of ZHX2, but not RCBTB2 or RAN, is associated with poor outcome in multiple myeloma. Br J Haematol 2008;141:212–215.
30. Liu G, Clement LC, Kanwar YS, et al. ZHX proteins regulate podocyte gene expression during the development of nephrotic syndrome. J Biol Chem 2006;281:39681–39692.
31. Rosenblatt J, Gu Y, Morgan DO. Human cyclin-dependent kinase 2 is activated during the S and G2 phases of the cell cycle and associates with cyclin A. Proc Natl Acad Sci U S A 1992;89:2824–2828.
32. Knoblich JA, Sauer K, Jones L, et al. Cyclin E controls S phase progression and its down-regulation during Drosophila embryogenesis is required for the arrest of cell proliferation. Cell 1994;77:107–120.
33. Legartova S, Harnicarova-Horakova A, Bartova E, et al. Expression of RAN, ZHX-2, and CHC1L genes in multiple myeloma patients and in myeloma cell lines treated with HDAC and Dnmts inhibitors. Neoplasma 2010;57:482–487.
34. Kramer A, Carstens CP, Wasserman WW, et al. CBP/cycA, a CCAAT-binding protein necessary for adhesion-dependent cyclin A transcription, consists of NF-Y and a novel Mr 115,000 subunit. Cancer Res 1997;57:5117–5121.
35. Jung YJ, Lee KH, Choi DW, et al. Reciprocal expressions of cyclin E and cyclin D1 in hepatocellular carcinoma. Cancer Lett 2001;168:57–63.

36. Morford LA, Davis C, Jin L, et al. The oncofetal gene glypican 3 is regulated in the postnatal liver by zinc fingers and homeoboxes 2 and in the regenerating liver by alpha-fetoprotein regulator 2. Hepatology 2007;46:1541–1547.
37. Vacher J, Camper SA, Krumlauf R, et al. raf regulates the postnatal repression of the mouse alpha-fetoprotein gene at the post-transcriptional level. Mol Cell Biol 1992;12:856–864.
38. Hoshida Y, Villanueva A, Kobayashi M, et al. Gene expression in fixed tissues and outcome in hepatocellular carcinoma. N Engl J Med 2008;359:1995–2004.

Received July 15, 2011. Accepted February 28, 2012.

AQ: 2 *Reprint requests*
Address requests for reprints to: Chunhong Ma, PhD, Key Laboratory for Experimental Teratology of Ministry of Education and Institute of Immunology, Shandong University School of Medicine, 44 Wenhua Xi Road, Jinan, Shandong 250012, People's Republic of China. e-mail: machunhong@sdu.edu.cn; fax: (86) 531-88382038. AQ: 37

Conflicts of interest AQ: 4
The authors disclose no conflicts. AQ: 3

Funding AQ: 5
This work was supported in part by grants from the National Natural Science Foundation of China (no. 30972753), the Programme for New Century Excellent Talents in University (no. NECT-10-0524), the Independent Innovation Foundation of Shandong University, the Shandong Provincial Nature Science Foundation for Distinguished Young Scholars (no. JQ200907); and the National Institutes of Health (grant DK95866 to B.T.S.). AQ: 6 AQ: 7

Supplementary Table 1. Primers Used in the Study

Primer name	Forward sequence	Reverse sequence
ZHX2(242–446)	GCGAATTCATGGTCATGCCTTCTGTACAGC	CCGGTACCTGTGAGCGGGGGGTTG
ZHX2(242–439)	GCGAATTCATGGTCATGCCTTCTGTACAGC	CCGGTACCCTTCTTGCGGTCACTGC
Cyc A ChIP	TCGCCAAGTTTATTCCGTTTA	CCGACGCTTCCGATTATTT
Cyc E ChIP	CCCGCCGTGTTTACATTCC	ACGCGGGAGAAGTCTGGC
Cyc D1 ChIP	CCTTGGGCATTTGCAACGAC	CGCATTTCCAAGAACGCC AC
Cyc A RT-PCR	TGAACTACATTGATAGGTTCCTGT	TGACTGTTGTGCATGCTGTGGTGC
Human *actin* RT-PCR	GGCATCGTGATGGACTCCG	GCTGGAAGGTGGACAGCGA
ZHX2 RT-PCR	CCCCCAATGGTGCTCTGT	TTGCTTTCCTTGCTACGG
Cyc E RT-PCR	CTCCAGGAAGAGGAAGGCAA	TCGATTTTGGCCATTTCTTCA
siCycA	CUACAUUGAUAGGUUCCUGTT	TTGAUUGUAACUAUCCAAGGAC
siCycE	CACCCUCUUCUGCAGCCAATT	TTGUGGGAGAAGACGUCGGUU
siCycD1	GUUCAUUUCCAAUCCGCCCTT	TTCAAGUAAAGGUUAGGCGGG

RT, reverse-transcription.

Supplementary Table 2. ZHX2 Nuclear Expression, Clinical, and Histologic Features in 82 Patients With HCC Used for This Study

			ZHX2 nucleus expression		
Clinical characteristic	Average (±SD)	Cases, n	Positive (4–12)	Negative (0–3)	Median ± SD (range)
Sex					
Female		10	8	2	4 ± 4.2 (0–12)
Male		72	39	33	4 ± 4.3 (0–12)
P value			.1767[a]		.2751[b]
Age, *y*					
≤50	42.2 ± 6.6	33	16	17	3 ± 4.6 (0–12)
<50	58.1 ± 6.4	49	28	21	4 ± 4.2 (0–12)
P value			.2644[a]		.4838[b]
HBeAg					
Positive		52	30	22	4 ± 4.5 (0–12)
Negative		24	13	11	4 ± 4.3 (0–12)
P value			.8074[a]		.3877[b]
HBsAg					
Positive		58	33	25	4 ± 4.4 (0–12)
Negative		17	10	7	4 ± 4.4 (0–12)
P value			.8877[a]		.2484[b]
Cirrhosis					
Positive		23	15	8	4 ± 4.3 (0–12)
Negative		59	29	30	3 ± 4.4 (0–12)
P value			.1900[a]		.2061[b]
AFP level, *ng/mL*					
≤20	6.22 ± 4.5	26	14	12	4 ± 3.5 (0–12)
<20	2556.68 ± 6052.22	44	27	17	4 ± 4.6 (0–12)
P value			.6188[a]		.0676[b]
Differentiation grade					
Poor		26	9	17	0 ± 3.1 (0–12)
Moderate		43	23	20	3 ± 3.8 (0–12)
Well		13	11	2	4 ± 2.8 (0–12)
P value			.0127[a]		.0006[c]

[a]*P* values of dispersion of ZHX2 staining were studied by the chi-square test.
[b]*P* values of median value of ZHX2 immunoreactivity were analyzed by the nonparametric test.
[c]*P* values of dispersion of ZHX2 staining were analyzed by the one-way ANOVA test.

Supplementary Table 3. ZHX2 Nuclear Expression in the Tissue Array With HCC Used for This Study

			ZHX2 nucleus expression		
	Average (±SD)	Cases, *n*	Positive (4–12)	Negative (0–3)	Median ± SD (range)
Sex					
Female		6	3	3	5.5 ± 5.2 (0–12)
Male		46	28	18	6 ± 4.6 (0–12)
P value			.6098[a]		.4622[b]
Age, *y*					
≤50	45 ± 3.9	16	7	9	3 ± 5.1 (0–12)
<50	56.5 ± 4.8	36	24	12	8 ± 4.4 (0–12)
P value			.1201[a]		.1674[b]
Cirrhosis					
Positive		25	15	10	9 ± 4.6 (0–12)
Negative		27	16	11	4 ± 4.8 (0–12)
P value			.9566[a]		.4320[b]
Differentiation grade					
Poor		11	2	9	2 ± 3.8 (0–12)
Moderate		30	19	11	8 ± 4.3 (0–12)
Well		10	9	1	12 ± 3.9 (3–12)
P value			.0028[a]		.0027[c]
All specimens					
Cancer		52	31	21	6 ± 4.6 (0–12)
Noncancer		54	47	7	8 ± 3.7 (0–12)
P value			.0014[a]		.0067[c]
Small tumor (≤5 cm)					
Cancer		25	13	12	4 ± 4.9 (0–12)
Noncancer		26	22	4	8 ± 3.5 (0–12)
P value			.0121[a]		.0915[c]

[a]*P* values of dispersion of ZHX2 staining were studied by the chi-square test.
[b]*P* values of median value of ZHX2 immunoreactivity were analyzed by the nonparametric test.
[c]*P* values of dispersion of ZHX2 staining were analyzed by the one-way ANOVA test.

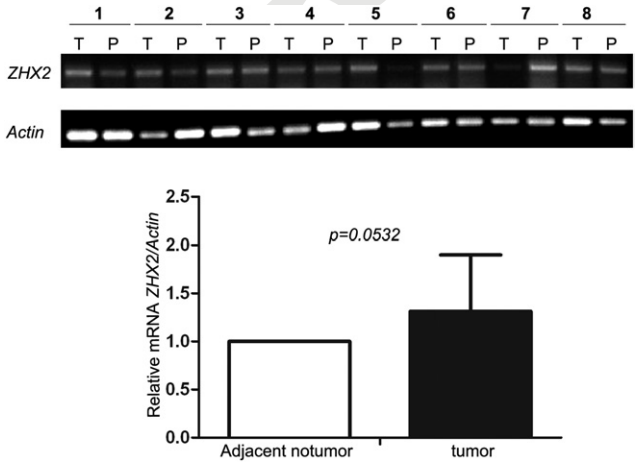

Supplementary Figure 1. The total RNA was extracted from liver tissues from patients with HCC. Reverse-transcription PCR was used to analyze the expression of ZHX2 in mRNA levels. *Top*: results of the gel electrophoresis; *bottom*: statistical results are shown.

AQ: 34